RSC Advances

ROYAL SOCIETY OF CHEMISTRY

www.rsc.org/advances

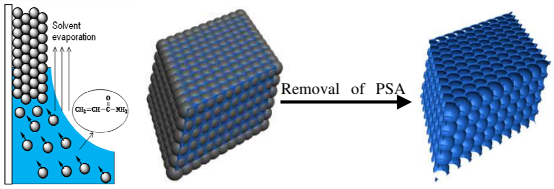

Exfoliated polyacrylamide (PAM) inverse opal film had been fabricated based on co-deposition motif.

Co-deposition Motif for Constructing Inverse Opal Photonic Crystals with pH Sensing

Zhaokun Yang, Dongjian Shi, Xiaodong Zhang, Huanhuan Liu, Mingqing Chen, and Shirong Liu*

The Key Laboratory of Food Colloids and Biotechnology, Ministry of Education, School of Chemical and Material Engineering, Jiangnan University, Wuxi 214122, P. R. China

Corresponding Author:

Shirong Liu, E-mail: liushirong1@aliyun.com.

Abstract

Polyacrylamide (PAM) hydrogel photonic crystals with inverse-opal structure were elaborated using modified vertical deposition approach, in which co-deposition motif was involved. Free-standing inverse opal hydrogel (IOH) film with different thicknesses that peeled from the supporters was firstly fabricated. Three-dimensional ordered structure without over-layers could easily be acquired assisted by the co-deposition approach. And the bi-continuous structure could not be affected with the increase of film thickness. All of these IOH films showed fascinating pH response property after hydrolysis, and the color change corresponding to the shift of Bragg diffraction peak of the acquired hydrogel photonic crystal films can be easily

distinguished by the naked eye. Three types of IOH films with different thicknesses showed similar pH response property. Co-deposition approach is suitable for the construction of the thicker IOH film without over-layers.

Keywords: Co-deposition; Inverse opal; Photonic crystal; pH sensing

Introduction

Hydrogel photonic crystals (HPCs) have attracted considerable interest due to the sensing to external stimuli, such as temperature, [1,2] pH, [3,4] ionic strength, [5] humidity, [6,7] mechanic forces [8,9] , metal ions [10,11] and molecules. [12,13] Generally, there are two fundamental types of HPCs, including polymerized crystalline colloidal array (PCCA) hydrogel photonic crystals [14] and inverse opal hydrogel (IOH) film deposited on a substrate. [15] PCCA hydrogel photonic crystals are formed through the immobilization of non-close-packed, three-dimensional highly ordered suspension crystalline colloidal array (CCA) in the polymer network via in situ polymerization. The PCCA system has the advantage of simplification of the fabrication process, whereas poor sensitivity and slow response, resulting from the mass transfer resistance of the polymer network, may limit the application in a real-world situation. Furthermore, PCCA system could be easily destroyed when introducing charged monomers into the pre-polymerization solution because of the CCA need to be stabilized by charge. [16] Fortunately, these issues of PCCA could be easily addressed by IOH with three dimensional highly ordered macroporous structure, which provides merits of highly

sensitive and rapid response and allows the employment of various kinds of charged monomers. [17-20]

It is well known that conventional fabrication method of IOH has generally been conducted in three-step templating process, including assembly of colloidal crystal template, the infiltration of precursors to the colloidal crystal template and the removal of colloidal crystal template. [21] Compared with PCCA, IOH possesses more complicated fabrication process, and thin film of IOH deposited on a substrate could not be peeled off easily. However, the adhesion to the substrate can affect the swelling or shrinking behavior of IOH film and thereby excellent responsive property that is imparted by the macroporous structure. [22] Therefore, it is highly desirable and useful to obtain free-standing IOH film in accordance with the formation of PCCA. It can be envisioned that free-standing IOH film could be acquired when the thickness of colloidal crystal template reaches certain level. Nevertheless, free-standing IOH film has never been demonstrated so far, probably due to the following difficulties. Firstly, the infiltration of precursors to the template could not easily be controlled when thick template is employed. Excessive infiltration would occur in this situation, resulting in the overlap of the surface of colloidal crystal template, and inverse opal structure can not be prepared owing to the failure of the removal of the colloidal particles. The overlapped area of IOH film can almost be considered as PCCA where lattice spacing is approximately equal to particle diameter itself. In such a case, excellent sensing property of IOH film with complex fabrication process no longer exist. On the other hand, colloidal crystal template produced via conventional methods, such as

sedimentation, [23] centrifugation, [24] spin-coating [25] and evaporative deposition, [26] bears many cracks, colloid vacancies and other defects. And much more defects formed with the increase of the thickness of the template and were harmful for the formation of ordered macroporous structure. Furthermore, three-step method for IOH film is much more sophisticated than that of PCCA. Therefore, it is urgent to develop a simple and efficient method that allows formation of free-standing IOH film. Co-assembly method has been proven to be effective for the preparation of silica inverse opal with crack-free and high order over centimeter length scales by Hatton group. [27] And our group has prepared organic inverse opal materials based on co-deposition approach combining in situ polymerization of PCCA with colloidal crystal template method. [28] However, fabricated inverse opal photonic crystals are deposited on a substrate, and the sensing property of that has not been investigated. It is necessary for the practical application to study the response of co-deposition based photonic crystal.

In this study, free-standing IOH films with different thicknesses were firstly demonstrated based on co-deposition motif, and phenomenon of overlap did not appear for various situations. The pH sensing property of free-standing IOH films with various thicknesses were investigated. The pH sensing behavior of free-standing IOH film can be accomplished between 5 and 10 seconds. Moreover, reciprocal sensing of free-standing IOH film was also elaborated, evidencing good physical stability and proper mechanical strength of IOH film.

Experimental

Materials

Acrylamide (AM), acrylic acid (AA), ammonium persulfate (APS), N,N,N',N'-tetramethylethylenediamine (TEMED) and Styrene were purchased from Sinopharm Chemical Reagent Co., Ltd. N,N'-methylene bisacrylamide (BIS) was obtained from Aladdin Chemistry Co., Ltd. (China). Styrene and AA were purified by distillation under vacuum. All other affiliated chemicals not mentioned here were used without further purification. Glass slides (76.2×24.5×1 mm) for colloidal crystal growth were well-cleaned using acetone, anhydrous ethanol and double-distilled water in an ultrasonic bath in succession.

Preparation of free-standing inverse opal hydrogel (IOH)

The monodispersed poly(styrene-co-acrylic acid) (PSA) colloids (~200 nm) were synthesized by emulsifier-free emulsion polymerization according to our previous work. Prior to fabrication of IOH, suspension solution was firstly obtained by adding 2 mL of pre-polymerization solution into 20 mL of x wt% colloidal suspensions, which take the value of 0.5, 1 or 2. The standard pre-polymerization solution was composed of AM (5.0 g), BIS cross-linker (0.5 g), APS (0.05 g) and H_2O (30.0 mL). Then a glass slide already mentioned was vertically dipped into the prepared suspension solution in the beaker. And then the beaker were placed in an oven at 50 ℃ for 28 h, accompanied by co-deposition of PSA microspheres and AM precursor on substrates and polymerization of AM precursor in a single step, and uncoated composite opal film was formed eventually. Continually, composite opal

film can be easily peeled off from the substrate through immersion in H_2O. After that free-standing IOH film (2.4 × 1.5 cm) with bright color was finally obtained through selectively removal of the PSA colloids by sintering in air at 100 ℃ for 0.5 h and subsequently dissolving in xylem solution (24 h) at room temperature. Eventually, the free-standing IOH film was immersed into a mixture of 0.1 M sodium hydroxide and 10 wt % TEMED. After 1 min of hydrolysis, the film was thoroughly washed with deionized water. Three types of IOH film with thicknesses of (a) ~25 μm, (b) ~50 μm and (c) ~90 μm, had been fabricated by changing the mass fraction of colloids suspended in suspension solution.

Characterization

Surface morphologies of composite opal film and IOH film were characterized by field emission scanning electron microscopy (SEM, Hitachi, S-4800). The pH-dependent Bragg diffraction wavelength of IOH was recorded by a miniature fiber optic spectrometer (FLA 4000+, China). The corresponding color changes were photographed using a common digital camera under a daylight lamp.

Results and discussion

Co-deposition based IOH film

A simple and novel co-deposition approach was employed to prepare free-standing IOH film as shown in Fig. 1. Co-deposition approach consists of only two steps of co-deposition of PSA microspheres and AM precursor on substrates and polymerization of AM precursor in a single process and PSA colloids removal. In the

first step, owing to hydrogen effects between the $–CONH_2$ groups of AM and –COOH groups of PSA particles, suspension solution exists in the form of AM surrounding the PSA particles. Accordingly, during evaporation-induced colloidal assembly, AM of a certain concentration can be homogeneously penetrated into interstitial between PSA colloids. And polymerization of precursor, reaching to the level of enabling polymerization, proceeded simultaneously with the assembly of colloids due to continuous evaporation of solvent. Secondly, free-standing IOH film was obtained by the removal of PSA colloids. The thickness of free-standing IOH film can be modulated by mass fraction of colloids suspended in suspension solution. The higher mass fraction of colloids was, the thicker film would be acquired.

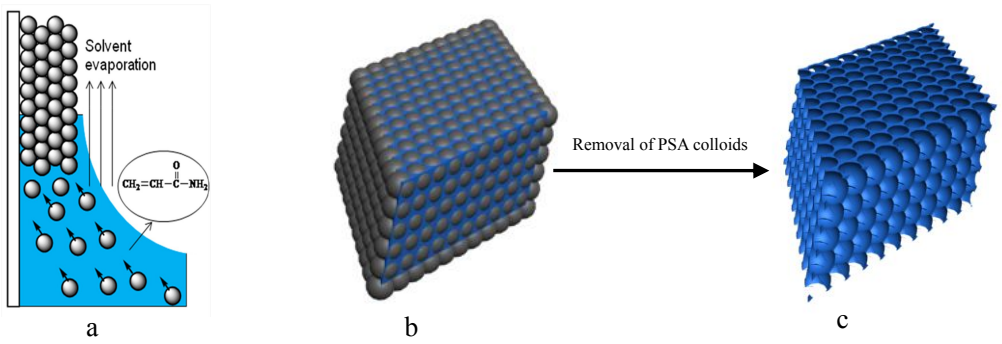

Fig. 1 (a) Schematic illustration of the co-deposition process. (b) Composite opals consisted of PSA colloids and PAM hydrogel. (c) PAM inverse opals.

Fig. 2 showed the typical SEM images of the resultant IOH film with different thicknesses. As it can been seen clearly, 3D highly ordered and interconnected macroporous arrays were fabricated successfully. And the ordered macroporous structure was relatively unaffected by the thickness. Herein, it can be asserted that co-deposition method is extraordinary suitable for the fabrication of nearly

overlayer-free free-standing IOH film. In a regular inverse opal structure, there are three pores that can be seen in each void.[29] In our work, a void had three or less than pores as shown in Fig. 2, and the problem of partially etching was not improved by increasing the etching time. The construction of perfect inverse opal structure would be an important part of our next research subjects. Although perfect inverse opal structures were not guaranteed, uncoated IOH film in the first layer could easily be fabricated by co-deposition approach. Moreover, IOH film based on co-deposition motif had addressed many other defects, such as cracks and overlapping.

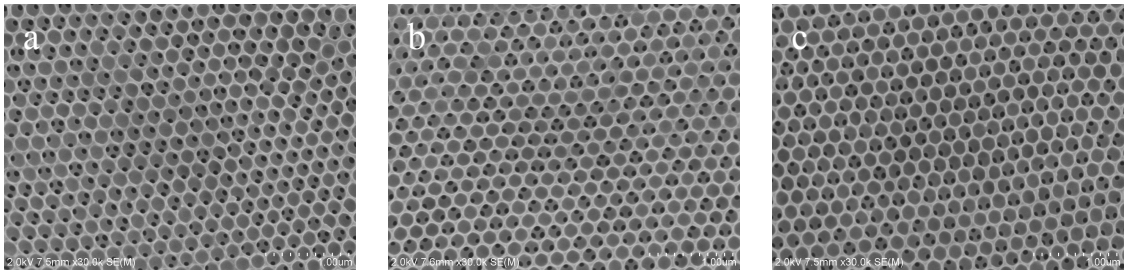

Fig. 2 SEM images of inverse opals film fabricated by various mass fraction of colloidal suspension: (a) 0.5%, (b) 1%, (c) 2 %.

pH response of IOH film

Fig. 3 presented the pH dependence of Bragg diffraction wavelength of IOH film with thicknesses of 90 μm in buffer solutions. It can be clearly seen that Bragg diffraction peak of IOH film shifted markedly from 467 nm to 550 nm when the pH was increased from 2.67 to 8.43. This resulted from the electrostatic repulsion among the carboxylate anions on the polymer chains and the increase of osmotic pressure. When the IOH film was hydrolyzed, some amide groups hydrolyzed to carboxyl groups, which would ionize as a function of the pH. As the pH increased from 2.67 to 8.43, ionization of the carboxyl groups were raising, resulting in the increase of the

carboxylate anions. The carboxylate anions on the polymer chains brought about an electrostatic repulsion which tends to expand the polymer network. Furthermore, osmotic pressure is also a key reason for the pH response of IOH film. According to the Flory-Rehner theory,[30-32] total osmotic pressure Π for ionic hydrogels is given as the sum of the pressures due to polymer-solvent mixing (mix), due to deformation of network chains to a more elongated state (el), and due to the nonuniform distribution of mobile counterions between the hydrogel and the external solution (ion):

$$\Pi = \Pi_{mix} + \Pi_{el} + \Pi_{ion}$$

In this paper, pH-dependent optical properties of IOH film are mainly related to Π_{ion}. With the increase of pH, the concentration difference of counterions between the hydrogel and the outer solution became larger. Therefore, the value of Π_{ion} increased, resulting in the increase of total osmotic pressure Π. The increase of osmotic pressure and electrostatic repulsion among molecular chains would swell the gel, and induce the redshift of Bragg diffraction peak. Then it was noteworthy that Bragg diffraction peak blue shifted with further pH increased. Since ionization was complete by pH 9, further pH would only increase ionic strength, which leaded to the decrease of osmotic pressure and would shrink the hydrogel. In addition, deionization of acylamino group occurred when the value of pH was greater than pKa (9.6) of acylamino group. That would also shrink the hydrogel and caused the buleshift of Bragg diffraction peak. Specially, pH response of IOH film with different thicknesses showed little difference. Therefore, thicker IOH film should be fabricated for the convenient employment in the real-world situation.

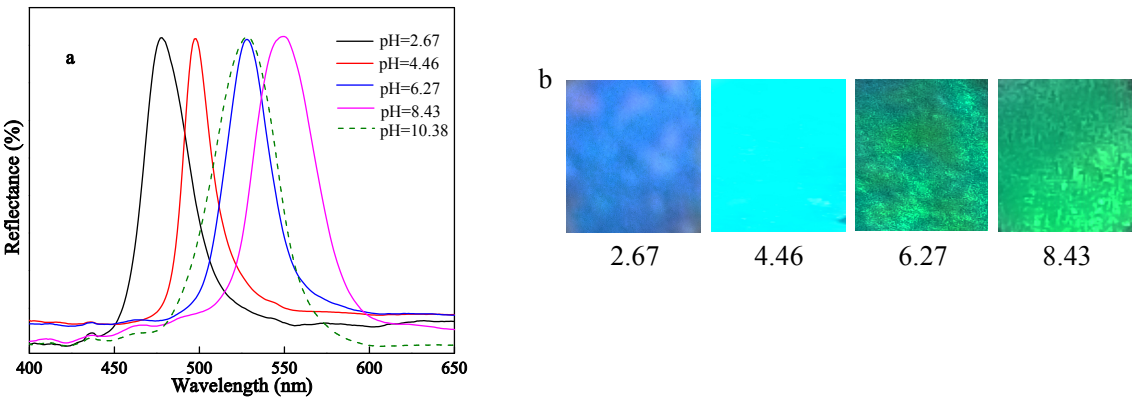

Fig. 3 (a) Optical response of IOH film upon soaking in buffer solutions at different pH values. (b) Photograph of IOH film under different pH conditions.

Response speed and recoverability of IOH film

Fig. 4 showed the pH responsive time of the IOH film with thicknesses of 90 μm upon soaking in solutions between pH 2.67 and pH 8.43. The response process was complete within 10 s. As the film thickness increased, the response speed was slightly slower. But relative fast response could still accomplished. The fast response may due to the 3D ordered interconnected macroporous structure and ultrathin hydrogel walls. In summary, pH response and response speed were not obviously influenced by the film thickness. However, the film thickness had exerted impact effect on the recoverability of IOH film. The IOH film would be mechanically more robust owing to the increase of film thickness. Fig. 5 exhibited the pH dependence of Bragg diffraction wavelength of IOH film based on 2 wt% colloidal suspensions when the pH varied from 2.67 to 10.38 with one cycle. Significant reciprocal response to pH was certified. Although similar phenomenon had been seen for other IOH films with different thicknesses, operation process needed to be very careful owing to the easily

damaged. The thicker film, which would not destroyed in process of test, is convenient for the practical employment.

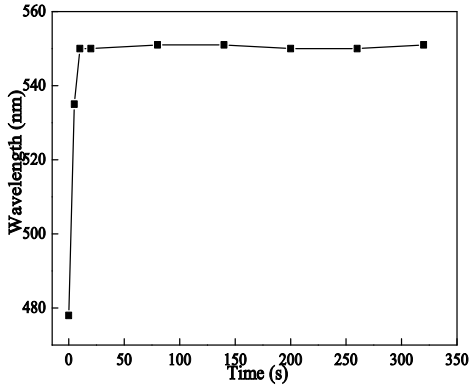

Fig. 4 Kinetic response of IOH film upon soaking in buffer solutions between pH 2.67 and pH 8.43.

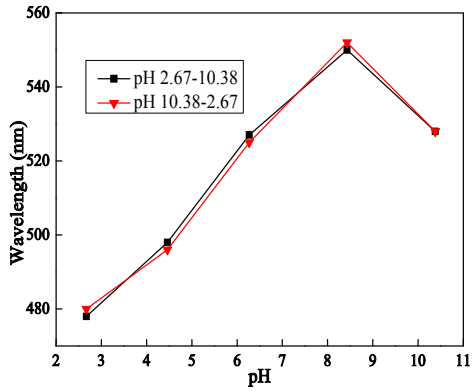

Fig. 5 Reciprocal sensing of PAM IOH film upon soaking in buffer solutions at different pH values.

Conclusions

In this study, PAM inverse opal films with different thicknesses have been successfully prepared by a simple co-deposition method. It has been proved that co-deposition approach is suitable for the construction of the thicker IOH film without over-layers. And the thickness has not weakened the pH response property of IOH

film, including respond speed and sensitivity. All of these IOH films have shown fascinating pH response property after hydrolyzed. The Bragg diffraction peak redshifted marked with the increase of pH in the range of 2.67 to 8.43. In contrast, with the increase of pH continually, the Bragg diffraction peak would blueshift. The pH sensing behavior of free-standing IOH film can be accomplished between 5 and 10 seconds. In summary, the thicker IOH film without over-layers can be acquired by the co-deposition approach. And the sensing property of IOH film is still extraordinary. Co-deposition method involved in the fabrication of polymer hydrogel photonic crystal would accelerate the process of practical application of photonic crystal.

Acknowledgements

This study was supported by the National Natural Science Foundation of China (No. 51173072), the Fundamental Research Funds for the Central Universities (JUSRP51408B), and MOE & SAFEA for the 111 Project (B13025).

References

1 H. Kawaguchi, *Polym Int*, 2014, **63**, 925-932.

2 H. R. Ma, M. X. Zhu, W. Luo, W. Li, K. Fang, F. Z. Mou and J. G. Guan, *J Mater Chem C*, 2015, **3**, 2848-2855.

3 C. Yao, J. Y. Ren, C. H. Liu, T. Yin, Y. X. Zhu and L. Q. Ge, *ACS applied materials & interfaces*, 2014, **6**, 16727-16733.

4 S. Pace, R. B. Vasani, W. Zhao, S. Perrier and N. H. Voelcker, *Nanoscale research letters*, 2014, **9**, 420-426.

5 C. Fenzl, S. Wilhelm, T. Hirsch and O. S. Wolfbeis, *ACS applied materials & interfaces*, 2013, **5**, 173-178.

6 Y. Z. Zhang, Z. R. Li, Y. M. Zheng, J. X. Wang, Y. L. Song and L. Jiang, *Acta Polym Sin*, 2010, 1253-1261.

7 H. B. Hu, Q. W. Chen, K. Cheng and J. Tang, *J Mater Chem*, 2012, **22**, 1021-1027.

8 L. M. Fortes, M. C. Goncalves and R. M. Almeida, *Opt Mater*, 2011, **33**, 408-412.

9 Y. F. Yue, T. Kurokawa, M. A. Haque, T. Nakajima, T. Nonoyama, X. F. Li, I. Kajiwara and J. P. Gong, *Nature communications*, 2014, **5**, 4659-4666.

10 M. L. Zhang, F. Jin, M. L. Zheng and X. M. Duan, *Rsc Adv*, 2014, **4**, 20567-20572.

11 Y. B. Baek, S. H. Choi and D. M. Shin, *Journal of nanoscience and nanotechnology*, 2015, **15**, 1624-1627.

12 K. I. MacConaghy, C. I. Geary, J. L. Kaar and M. P. Stoykovich, *Journal of the American Chemical Society*, 2014, **136**, 6896-6899.

13 T. Tian, X. Li, J. Cui, J. Li, Y. Lan, C. Wang, M. Zhang, H. Wang and G. Li, *ACS applied materials & interfaces*, 2014, **6**, 15456-15465.

14 S. A. Asher, J. Holtz, L. Liu and Z. J. Wu, *Journal of the American Chemical Society*, 1994, **116**, 4997-4998.

15 Y. J. Lee and P. V. Braun, *Advanced materials*, 2003, **15**, 563-566.

16 Q. Cui, W. Wang, B. Gu and L. Liang, *Macromolecules*, 2012, **45**, 8382-8386.

17 W. Hong, Y. Chen, X. Feng, Y. Yan, X. B. Hu, B. Y. Zhao, F. Zhang, D. Zhang, Z.

Xu and Y. J. Lai, *Chem Commun*, 2013, **49**, 8229-8231.

18 J. J. Bohn, M. Ben-Moshe, A. Tikhonov, D. Qu, D. N. Lamont and S. A. Asher, *Journal of colloid and interface science*, 2010, **344**, 298-307.

19 Z. H. Zhang and H. J. Wu, *Chem Commun*, 2014, **50**, 14179-14182.

20 I. Tokarev and S. Minko, *Advanced materials*, 2010, **22**, 3446-3462.

21 Y. Liu, Y. X. Yuan, J. K. Ma, Y. Liu, L. Cui, R. G. Huang and J. P. Gao, *J Mater Chem*, 2011, **21**, 19233-19240.

22 N. Griffete, H. Frederich, A. Maitre, S. Ravaine, M. M. Chehimi and C. Mangeney, *Langmuir*, 2012, **28**, 1005-1012.

23 D. A. Eurov, D. A. Kurdyukov, E. Y. Trofimova, S. A. Yakovlev, L. V. Sharonova, A. V. Shvidchenko and V. G. Golubev, *Phys Solid State+*, 2013, **55**, 1718-1724.

24 M. Chen, H. Colfen and S. Polarz, *Z Naturforsch B*, 2013, **68**, 103-110.

25 Z. H. Hu, C. A. Tao, F. Wang, X. R. Zou and J. F. Wang, *J Mater Chem C*, 2015, **3**, 211-216.

26 C. Q. Zhou, X. X. Gong, J. Han and R. Guo, *Soft Matter*, 2015, **11**, 2555-2562.

27 B. Hatton, L. Mishchenko, S. Davis, K. H. Sandhage and J. Aizenberg, *P Natl Acad Sci USA*, 2010, **107**, 10354-10359.

28 H. Liu, D. Shi, F. Duan, Z. Yang, M. Chen and S. Liu, *Mater Lett*, 2015, **150**, 5-8.

29 X. Zhang and G. J. Blanchard, *ACS applied materials & interfaces*, 2015, **7**, 6054-6061.

30 P. J. Flory and J. Rener, *J Chem Phys*, 1943, **11**, 521-526.

31 M. Xu, A. V. Goponenko and S. A. Asher, *Journal of the American Chemical*

Society, 2008, **130**, 3113-3119.

32 K. Lee and S. A. Asher, *Journal of the American Chemical Society*, 2000, **122**, 9534-9537.